

# Fractional squeezing: spectra and dynamics from generalized squeezing Hamiltonian with fractional orders

Sahel Ashhab<sup>1,2</sup>

<sup>1</sup>*Advanced ICT Research Institute, National Institute of Information and Communications Technology (NICT), 4-2-1, Nukui-Kitamachi, Koganei, Tokyo 184-8795, Japan*

<sup>2</sup>*Research Institute for Science and Technology, Tokyo University of Science, 1-3 Kagurazaka, Shinjuku-ku, Tokyo 162-8601, Japan*

## Abstract

We generalize the generalized-squeezing problem to include fractional values of the squeezing order  $n$ . This approach allows us to determine the locations of critical points at which qualitative changes in behaviour occur and accurately predict the behaviour at these critical points, which are challenging for conventional computational methods. Based on our numerical calculations, we identify with a high degree of confidence the point at which the spectrum turns from continuous to discrete and the point at which oscillations turn from having asymptotically infinite amplitudes to finite amplitudes. Furthermore, we numerically investigate the behaviour in the large  $n$  regime and provide an intuitive explanation that coincides with the numerical results.

## I. INTRODUCTION

Nonlinear interactions in quantum optics are expected to enable a number of new protocols for manipulating quantum systems [1–3]. Squeezing, in which photons are generated in pairs, has been extensively analyzed in numerous theoretical studies, and it has been realized in a variety of experimental setups. Generalized squeezing, in which photons are generated in multiples of  $n$  photons, is gaining increasing attention in recent years, spurred in part by the rapid recent advances in developing higher-order nonlinear interactions in various quantum technology platforms, such as superconducting circuits [4–7] and trapped ions [8, 9].

While generalized squeezing might at first sight look like a straightforward generalization of two-photon squeezing, it turns out to be much more difficult to model than two-photon squeezing [10–16]. These difficulties are highlighted in the contradicting conclusions of recent studies on the subject [17–21].

One of the interesting aspects of generalized squeezing observed in the simulations of Ref. [17] is the qualitative differences in behaviour for different squeezing orders. Some of the changes are counter-intuitive. For example, while the number of photons grows indefinitely and approaches infinity in the infinite-time limit for two-photon squeezing ( $n = 2$ ), the photon number diverges at a finite time for tri-squeezing ( $n = 3$ ), and the photon number remains finite at all times for quint-squeezing ( $n = 5$ ). Such disparate behaviour makes it highly desirable to have a better understanding of how the evolution between different squeezing orders happens.

While the squeezing order is an integer, we show in this paper that calculations can be set up in which the squeezing order can take any real-number value in a range that covers all integers from 1 to infinity. These calculations give us a closer view of how the behaviour changes as we change the squeezing order. Furthermore, it provides more certainty about the behaviour in certain cases than what we would obtain by analyzing integer values only. One example is the continuity of the spectrum in the case of two-photon squeezing. While the simulations in Ref. [19] were inconclusive, our results here provide stronger evidence that the spectrum is continuous, which is consistent with the well-known behaviour of two-photon squeezing dynamics.

The remainder of this paper is organized as follows. In Section II, we describe the

theoretical background and methodology of our numerical calculations. In Sec. III, we present the results of our numerical simulations and discuss some of their implications, such as the boundary between continuous and discrete spectra and the amplitude of generalized-squeezing oscillations. We discuss a few additional aspects of the results in Sec. IV, such as the asymptotic behaviour at large values of the squeezing order. We give some final remarks in Section V.

## II. THEORETICAL BACKGROUND AND COMPUTATIONAL METHODOLOGY

The generalized squeezing operator with squeezing order  $n$  is given by

$$\hat{U}_n(r) = \exp\left\{-ir\hat{H}_n\right\}, \quad (1)$$

where the squeezing Hamiltonian

$$\hat{H}_n = i\left[\left(\hat{a}^\dagger\right)^n - \hat{a}^n\right], \quad (2)$$

$r$  is the squeezing parameter, and  $\hat{a}$  and  $\hat{a}^\dagger$  are, respectively, the photon annihilation and creation operators.

As discussed for example in Ref. [20], the squeezing Hamiltonian is generally not essentially self-adjoint, and extra care must be taken when performing various operations on it to predict the behaviour of a physical system undergoing generalized squeezing dynamics. In this work we will focus on truncated versions of the operator and therefore not worry about the subtle mathematical questions related to self-adjointness, since these questions are not related to the main purpose of this work. Furthermore, we will focus on the squeezed vacuum state  $|\psi_n(r)\rangle$ , which is obtained by applying the squeezing operator to the vacuum (i.e. zero-photon) state  $|0\rangle$ :

$$|\psi_n(r)\rangle = \hat{U}_n(r)|0\rangle. \quad (3)$$

The relevant basis that contains the vacuum state is  $\{|0\rangle, |n\rangle, |2n\rangle, \dots\}$ . The Hamil-

nian for this space can be expressed in matrix form as

$$\hat{H}_n = \begin{pmatrix} 0 & -i\sqrt{n!} & 0 & 0 & \dots \\ i\sqrt{n!} & 0 & -i\sqrt{\frac{(2n)!}{n!}} & 0 \\ 0 & i\sqrt{\frac{(2n)!}{n!}} & 0 & -i\sqrt{\frac{(3n)!}{(2n)!}} \\ 0 & 0 & i\sqrt{\frac{(3n)!}{(2n)!}} & 0 \\ \vdots & & & \ddots \end{pmatrix}. \quad (4)$$

As mentioned above, we would like to analyze the evolution of various quantities as we gradually vary the squeezing order  $n$ . For this purpose, we rewrite Eq. (4) in the equivalent alternative form

$$\hat{H}(n) = \begin{pmatrix} 0 & -i\sqrt{\frac{\Gamma(n+1)}{\Gamma(1)}} & 0 & 0 & \dots \\ i\sqrt{\frac{\Gamma(n+1)}{\Gamma(1)}} & 0 & -i\sqrt{\frac{\Gamma(2n+1)}{\Gamma(n+1)}} & 0 \\ 0 & i\sqrt{\frac{\Gamma(2n+1)}{\Gamma(n+1)}} & 0 & -i\sqrt{\frac{\Gamma(3n+1)}{\Gamma(2n+1)}} \\ 0 & 0 & i\sqrt{\frac{\Gamma(3n+1)}{\Gamma(2n+1)}} & 0 \\ \vdots & & & \ddots \end{pmatrix}. \quad (5)$$

While the factorial function is defined only for non-negative integers, the gamma function is defined for all real numbers. We can therefore treat  $n$  as a continuous variable that can take any positive value (or, in principle, even negative values for which the gamma function is finite). In other words, the squeezing order  $n$  is no longer confined to integer values.

There is a serious conceptual issue with allowing  $n$  to take fractional values. When  $n$  is an integer, we can intuitively understand the Hamiltonian matrix as describing processes in which  $n$  photons are created or annihilated. When  $n$  is a fractional number, there is no simple, intuitive way to describe the Hamiltonian matrix, or even the basis, in physical terms. We therefore treat it simply as a mathematical tool that allows us to analyze the changes in various quantities as we gradually vary the squeezing order  $n$ .

We should mention here the field of fractional calculus, in which one can take fractional derivatives, as opposed to simply taking the first derivative, second derivative, etc. [22, 23]. There could be methods and results in the field of fractional calculus that can be applied to the present problem. However, since this endeavour can lead to involved mathematical techniques, we will not pursue it in the present work. It is also worth mentioning here the somewhat related idea of treating the number of spatial dimensions as a variable parameter

that can take any value, including fractional ones [24]. Some calculations are then simplified by first treating the infinite-dimension limit and then using the results as a starting point to investigate three-dimensional systems.

Our simulations proceed as follows: We construct a truncated Hamiltonian matrix of size  $N \times N$ . We always choose even values of  $N$ . To obtain the spectrum, we diagonalize this truncated Hamiltonian. As discussed in Ref. [19], the two eigenvalues that are closest to zero (and located symmetrically on the positive and negative sides of zero) contain important information, for example whether the spectrum is continuous or discrete in the limit of infinite  $N$ . For questions related to the dynamics, considering the spectral decomposition of the squeezing operator and the fact that the vacuum state is typically well approximated by a superposition of only the two eigenstates of the Hamiltonian that corresponds to one of the above-mentioned eigenvalues, we analyze these eigenstates. For the purpose of analyzing the dependence on  $n$ , we perform simulations for  $n = 0, 0.1, 0.2, \dots, 6$ .

In our analysis, we will define the renormalized number operator

$$\hat{m} = \begin{pmatrix} 0 & 0 & 0 & 0 & \dots \\ 0 & 1 & 0 & 0 & \\ 0 & 0 & 2 & 0 & \\ 0 & 0 & 0 & 3 & \\ \vdots & & & & \ddots \end{pmatrix}. \quad (6)$$

For integer squeezing orders  $n$ , the usual photon number operator  $\hat{a}^\dagger \hat{a}$  is related to  $\hat{m}$  by the formula  $\hat{a}^\dagger \hat{a} = n\hat{m}$ . Even though the two operators have this simple relation, the renormalized operator provides a conceptual simplification when dealing with fractional values of  $n$ , as well as the case  $n = 0$ . In the case  $n = 0$ , the basis states are all separated by zero photons, and the off-diagonal matrix elements in the Hamiltonian create or annihilate zero photons, such that the number of photons is always equal to zero, regardless of the quantum state. Therefore, analyzing the operator  $\hat{m}$  obviously provides more information than analyzing the operator  $n\hat{m}$ , which is always equal to zero. The expectation value  $\langle \hat{m} \rangle = \langle \psi_n^{(N)}(r) | \hat{m} | \psi_n^{(N)}(r) \rangle$  will be one of the main quantities that we will analyze below. We will also use the quantity  $n \langle \hat{m} \rangle$ , which we will also express as  $\langle \hat{a}^\dagger \hat{a} \rangle$  to provide an intuitively clear presentation of the results.

### III. SIMULATION RESULTS

We now present the results of the simulations described in Sec. II.

#### A. Continuity of spectrum

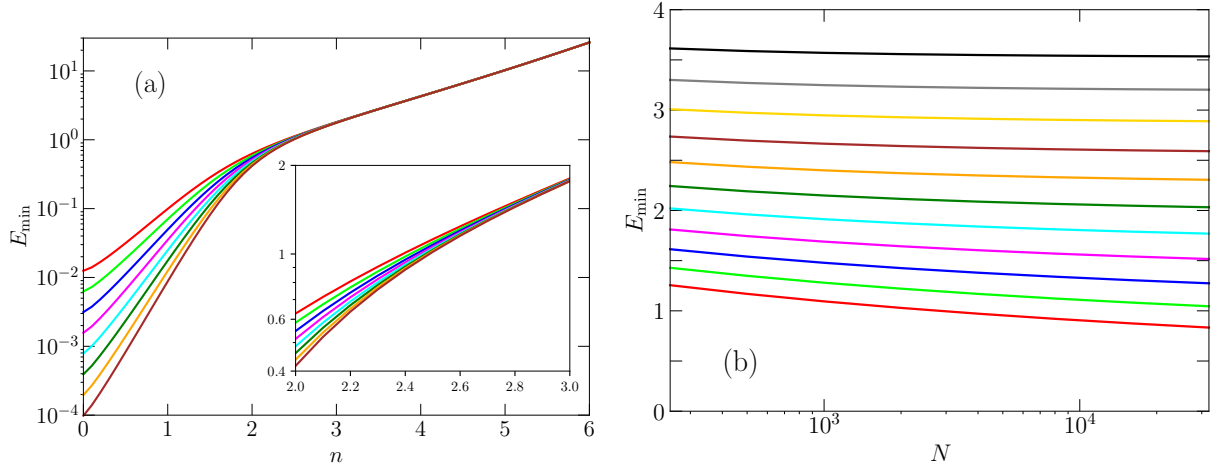


FIG. 1: (a) Smallest positive eigenvalue of the Hamiltonian  $\hat{H}(n)$ , which we denote as  $E_{\min}$ , as a function of the squeezing order  $n$ . The different lines (from top to bottom, i.e. red, green, blue, ...) correspond to to truncation sizes  $N = 250, 500, 1000, \dots, 250 \times 2^7$ . The inset zooms in on the range  $2 \leq n \leq 3$ . The progression of these lines shows that for small values of  $n$  (visually,  $n \lesssim 2$ ), the eigenvalue has not converged yet and appears to have the asymptotic values zero, while for large values of  $n$  ( $n \gtrsim 3$ ) the eigenvalue has clearly converged to its asymptotic value. As a further visual depiction of the convergence behaviour, Panel (b) shows  $E_{\min}$  as a function of the Hamiltonian truncation size  $N$  for  $n = 2, 2.1, 2.2, \dots, 3$  (bottom to top, i.e. red, green, blue, ...).

We start with the question of whether the spectrum is continuous or discrete. In Fig. 1(a), we plot the smallest positive eigenvalue of the Hamiltonian  $\hat{H}(n)$ , which we denote as  $E_{\min}$ , as a function of the squeezing order  $n$ . At the extreme point  $n = 0$ , it is clear that  $E_{\min}$  decreases by the same factor every time we double  $N$ , which implies that  $E_{\min} \propto N^{-\alpha}$  with some exponent  $\alpha$ . As such, the asymptotic value of  $E_{\min}$  in the limit  $N \rightarrow \infty$  is zero, and the spectrum is continuous in this limit. At the opposite extreme ( $n = 6$ ), the spectrum barely changes as we increase  $N$  from 250 to  $250 \times 10^7$ , indicating that the spectrum is discrete. In the intermediate region, roughly from  $n = 2$  to  $n = 3$ , the behaviour is not completely clear

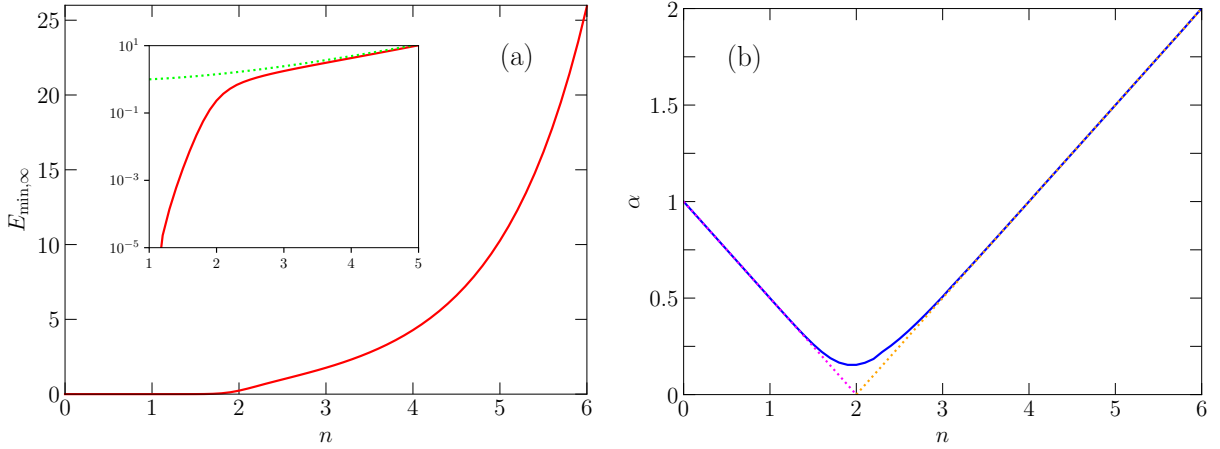


FIG. 2: (a) The asymptotic value of  $E_{\min}$ , obtained by extrapolating the data in Fig. 1 to  $N \rightarrow \infty$  and denoted by  $E_{\min,\infty}$ , as a function of the squeezing order  $n$ . Starting from  $n = 0$ ,  $E_{\min,\infty}$  remains essentially at zero up to around  $n = 2$ , after which it rises rapidly. The dependence of  $E_{\min,\infty}$  on  $n$  is examined further in the inset, which uses a logarithmic scale for the  $y$  axis. The green line is given by  $\sqrt{\Gamma(n+1)}$ , i.e. the smallest nonzero matrix element in the Hamiltonian. We will explain in Sec. IV why this function gives the asymptotic value of  $E_{\min,\infty}$  in the large- $n$  limit. (b) The exponent  $\alpha$  obtained from fitting the  $(N, E_{\min})$  data to the function in Eq. (7). Away from  $n = 2$ ,  $\alpha$  clearly follows linear functions of  $n$ , one for  $n < 2$  and one for  $n > 2$ . The linear dependence is represented by the dotted lines. As we approach  $n = 2$ , we see deviations from the linear functions. This deviation is likely caused by the inevitable numerical errors in our finite numerical simulations. Both linear functions go through the point  $(n = 2, \alpha = 0)$  when extrapolated.

from a visual inspection of Fig. 1 alone. To have a better visual view of the convergence behaviour in the region  $2 \leq n \leq 3$ , we plot  $E_{\min}$  as a function of  $N$  in Fig. 1(b). We can see that there is a trend towards a larger asymptotic value as we increase  $n$ , but we cannot make a definite conclusion about the asymptotic value for each curve, especially near  $n = 2$ .

Next we perform a fitting of the  $(N, E_{\min})$  data (with a fixed value of  $n$  for each data set) to the function

$$E_{\min} = E_{\min,\infty} + \delta E_{\min} \times N^{-\alpha}. \quad (7)$$

The constant term ( $E_{\min,\infty}$ ) is the asymptotic value of  $E_{\min}$  in the limit  $N \rightarrow \infty$ , while the exponent  $\alpha$  quantifies how fast  $E_{\min}$  approaches its asymptotic value. The results are shown

in Fig. 2. The asymptotic value  $E_{\min,\infty}$  is zero from  $n = 0$  all the way up to slightly below  $n = 2$ . For  $n > 2$ ,  $E_{\min,\infty}$  increases rapidly and approaches the function  $\sqrt{\Gamma(n+1)}$ , which is the smallest nonzero matrix element in the Hamiltonian. We will discuss in Sec. IV the reason why this function describes this asymptotic behaviour of  $E_{\min,\infty}$ . It is worth noting that the large- $n$  limit of this function is given by Stirling's formula:

$$\Gamma(n+1) \sim \sqrt{2\pi n} \left(\frac{n}{e}\right)^n, \quad (8)$$

which increases super-exponentially as a function of  $n$ . The exponent  $\alpha$  starts off at  $\alpha = 1$  when  $n = 0$ , then decreases linearly as a function of  $n$  in the direction of the point  $(n = 2, \alpha = 0)$ . Slightly before reaching  $n = 2$ , the line bends and does not reach exactly  $\alpha = 0$ . This result is natural, considering that  $\alpha = 0$  would be obtained from the fitting procedure if  $E_{\min}$  does not change with increasing  $N$ , and no such situation is encountered in the data. When  $n$  is sufficiently larger than 2,  $\alpha$  follows a linearly increasing function of  $n$ . Upon extrapolation, both linear functions that accurately describe  $\alpha$  well below and well above  $n = 2$  predict that  $\alpha = 0$  at  $n = 2$ . Taking the two panels of Fig. 2 together, we can infer that  $E_{\min,\infty}$  is likely to be equal to zero for all values of  $n$  between  $n = 0$  and  $n = 2$ , with a sub-polynomial scaling law governing  $E_{\min}$  as a function of  $N$  exactly at  $n = 2$ . The deviation of our results from this scenario can be attributed to numerical errors in our finite simulations.

## B. Quantum state size

We now analyze the expectation value of the renormalized photon number operator  $\langle \hat{m} \rangle$  for the eigenstate that corresponds to the smallest positive eigenvalue, i.e.  $E_{\min}$ . This quantity describes the size, or spread, of the quantum state. It is also closely related to the oscillation amplitude in the dynamics for  $n > 2$ , where the squeezing dynamics exhibits oscillations [17]. Specifically, the photon number oscillation amplitude is  $2n \langle \hat{m} \rangle$ , up to corrections from smaller, fast-oscillating terms.

Figure 3 shows that  $\langle \hat{m} \rangle$  decreases monotonically as a function of  $n$  for any given value of  $N$ . At the extreme point  $n = 0$ ,  $\langle \hat{m} \rangle = N/2$ . This result can be intuitively understood by noting the fact that all the nonzero matrix elements in the Hamiltonian  $\hat{H}(0)$  are equal, and there is a mirror symmetry between low and high number states. If we fix  $n$  somewhere in

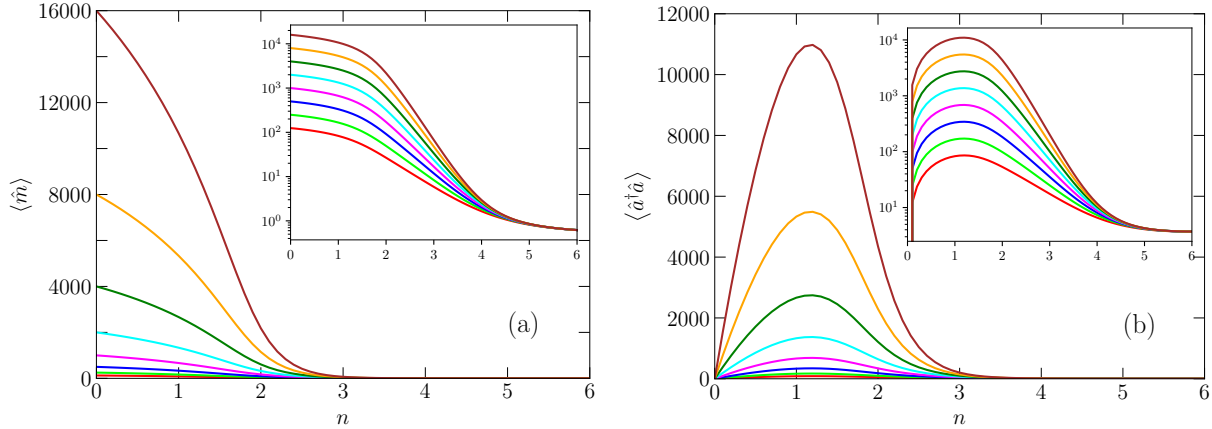


FIG. 3: (a) Expectation value of the renormalized photon number operator  $\langle \hat{m} \rangle$  for the eigenstate that corresponds to the eigenvalue  $E_{\min}$  as a function of squeezing order  $n$ . Panel (b) is a similar plot for the operator  $n\hat{m}$ , which we express as the usual photon number operator  $\hat{a}^\dagger\hat{a}$ . Both panels show that the plotted quantities seem to increase indefinitely as functions of  $N$  when  $n < 4$ . When  $n > 5$ , there is no discernible dependence on  $N$  for our simulation data, in which  $N$  covers the range  $[250, 250 \times 2^7]$ . The functional dependence is analyzed in more detail in Figs. 4 and 5.

the range  $0 \leq n \leq 4$  and increase  $N$ , we see that  $\langle \hat{m} \rangle$  increases indefinitely. This behaviour is seen more clearly in Figs. 4 and 5. The data in Figs. 3 and 4 is fitted well by the function

$$\langle \hat{m} \rangle = A \times N^{-\alpha} + B. \quad (9)$$

The exponent  $-\alpha$ , shown in Fig. 5, exhibits three different types of behaviour, which separates the set of all  $n$  values into three regimes.  $\alpha$  remains constant ( $\alpha = -1$ ) from  $n = 0$  to  $n = 2$ . Between  $n = 2$  and  $n = 4$ ,  $\alpha$  increases linearly towards  $\alpha = 0$  at  $n = 4$ . This trend indicates that the scaling law slows down as  $n$  increases. Exactly at  $n = 4$ , the fitting fails and generates an error in our numerical fitting calculations. The reason is that the data follows a logarithm scaling law, as shown in Ref. [17], and here we try to fit it with a power-law function. When  $n > 4$ , the  $(N, \langle \hat{m} \rangle)$  data have finite asymptotic values, which translates into positive values of  $\alpha$ . It is interesting that the straight lines below and above  $n = 4$  follow the same function, even though there is a qualitative change in behaviour at  $n = 4$ . The scaling prefactor plotted in Fig. 5(a) decreases from  $n = 0$  to  $n = 2$  and then increases from  $n = 2$  to  $n = 4$ . It should be noted that for  $n \leq 2$  the squeezing dynamics is expected to exhibit a monotonic increase in the photon number, while the dynamics is

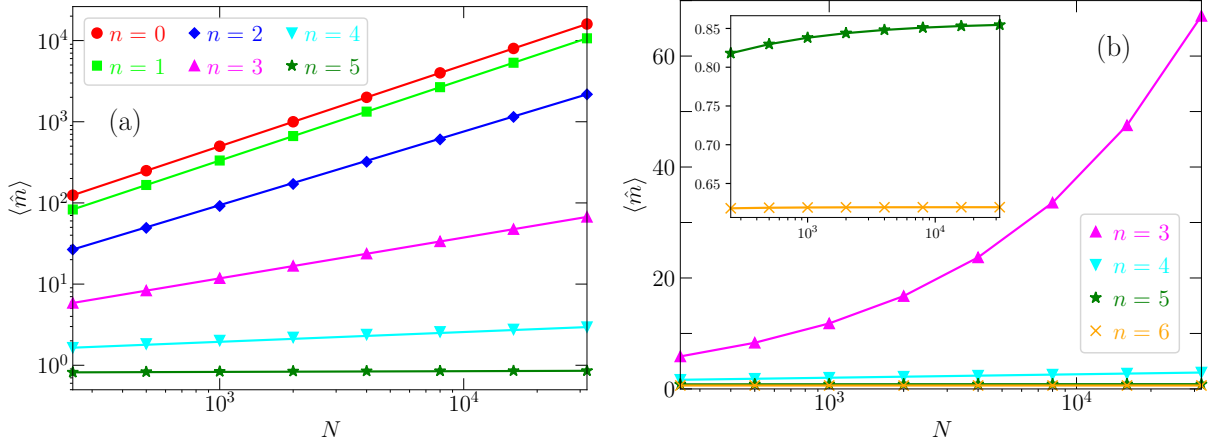


FIG. 4:  $\langle \hat{m} \rangle$  as a function of the truncation size  $N$  for a few values of  $n$ . Panel (a) shows the data in a log-log plot, while Panel (b) shows the data in a log-linear plot. Both panels show that  $\langle \hat{m} \rangle$  increases indefinitely as a function of  $N$  up to  $n = 4$ , while it converges to a finite value when  $n = 5, 6$ . The fact that each data set up to  $n = 3$  follows a straight line in the log-log plot indicates that the data follows a power law. The case  $n = 4$  was analyzed in Ref. [17], where it was found that the scaling is logarithmic. The logarithmic scaling cannot be seen clearly in this figure. The inset in Panel (b) shows that  $\langle \hat{m} \rangle$  converges to finite values for  $n = 5, 6$ . This point will be shown more clearly in Fig. 5.

expected to exhibit oscillations for  $n > 2$ , which would complicate any comparison in the behaviour of the parameter  $A$  across the two regions. Furthermore, for  $n < 2$ , the vacuum state has non-negligible overlap with a large number of eigenstates, such that the properties of the two eigenstates at the middle of the spectrum do not provide a sufficient description of the dynamics. Note also that the increase in  $A$  from  $n = 2$  to  $n = 4$  is accompanied by an increase in  $\alpha$ , such that the oscillation amplitude  $2n \langle \hat{m} \rangle$  ends up being a monotonically decreasing function of  $n$ , as can be seen by looking at the  $n > 2$  region in Fig. 3(b). As will be discussed in Sec. IV, the parameter  $B$  approaches the value 0.5 for large  $n$ , which confirms the observation in Ref. [17] that the oscillation amplitude stabilizes for  $n \geq 5$ .

#### IV. DISCUSSION

The results presented in Sec. III indicate a trend towards simple asymptotic behaviour in the large- $n$  limit. Specifically,  $E_{\min, \infty}$  approaches  $\sqrt{\Gamma(n+1)}$  and the parameter  $B$  in Fig. 5

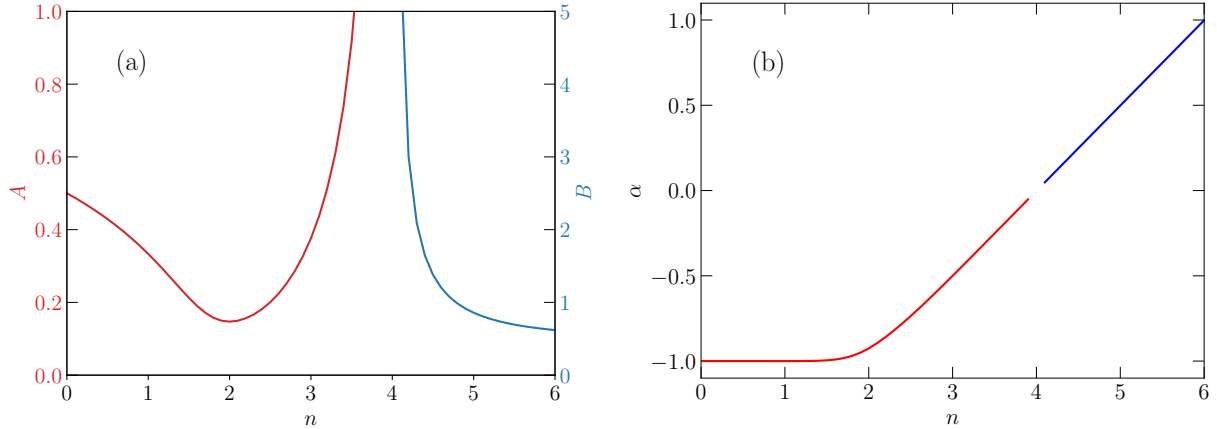


FIG. 5: Fitting parameters obtained by fitting the  $(N, \langle \hat{m} \rangle)$  data to the function  $A \times N^{-\alpha} + B$ . As can be seen in Panel (b), the exponent  $\alpha$  remains essentially constant from  $n = 0$  to  $n = 2$ . Then it increases linearly. The line interruption and change in color at  $n = 4$  signal that the point  $n = 4$  represents a demarcation point. When  $n < 4$ ,  $\alpha$  is negative, which means that  $\langle \hat{m} \rangle$  increases indefinitely and has the asymptotic value infinity. When  $n > 4$ ,  $\alpha$  is positive, which means that  $\langle \hat{m} \rangle$  approaches a finite asymptotic value. For this reason, it makes sense to focus on the parameter  $A$  (i.e. the scaling prefactor) for  $n < 4$  and to focus on the parameter  $B$  (i.e. the asymptotic value) for  $n > 4$ , as shown in Panel (a). The parameter  $B$  approaches 0.5 in the large- $n$  limit, as will be discussed in Sec. IV.

approaches 0.5. These results are what we would obtain if we truncate the Hamiltonian at  $N = 2$  and ignore all basis states except the first two. An intuitive understanding of this situation can be achieved by considering the artificial but instructive Hamiltonian

$$\hat{H}_{\text{hierarchical}} = \begin{pmatrix} 0 & h_2 & 0 & \cdots & 0 & 0 \\ h_2 & 0 & h_3 & & 0 & 0 \\ 0 & h_3 & 0 & & 0 & 0 \\ \vdots & & \ddots & & & \vdots \\ 0 & 0 & 0 & & 0 & h_N \\ 0 & 0 & 0 & \cdots & h_N & 0 \end{pmatrix}, \quad (10)$$

where  $h_j$  are all real and positive, and  $h_2 \ll h_3 \ll \cdots \ll h_N$ . If we focus on the highest two Fock states, they are coupled in the Hamiltonian by the pair of matrix elements equal to  $h_N$ . As a result, the Hamiltonian has a pair of large (positive and negative) eigenvalues approximately given by  $\pm h_N$ . The corresponding eigenvectors are, to a good approximation,

localized at the two highest states in the Fock space. All other matrix elements in the Hamiltonian are much smaller than  $h_N$ . Because of the energy mismatch, the two states with energies  $\pm h_N$  are almost completely decoupled from the rest of the Hilbert space. We can therefore remove them from the Hamiltonian, if we are considering dynamics and spectra that do not reach the energy scale of  $h_N$ . Furthermore, considering that all eigenvectors must be orthogonal to each other, the  $(N - 2)$  remaining eigenvectors must have a small total weight in the highest two Fock states. We can therefore restrict ourselves to the state space extending from 1 to  $N - 2$ , as the two highest states will not play a role near the middle of the spectrum. We can then repeat the same procedure and gradually remove pairs of eigenvalues from the spectrum until we are left with one or two eigenvalues at the center of the spectrum, depending on whether  $N$  is odd or even. The last remaining eigenvectors must be mostly confined to the lowest one or two Fock states. We have performed numerical simulations with matrix sizes ranging from  $2 \times 2$  to  $8 \times 8$  and with  $h_{j+1}/h_j = 10$  or  $100$  and confirmed that the spectrum follows the pattern explained above, i.e. forming energy level pairs with energies  $\pm h_N$ ,  $\pm h_{N-2}$ ,  $\pm h_{N-4}$  etc. When  $N$  is even, the last two eigenvalues in the middle of the spectrum will be given by  $\pm h_2$ , and the corresponding eigenvectors will be equal superpositions of the two lowest Fock states. When  $N$  is odd, the last remaining eigenvalue is unpaired and exactly equal to zero, with an eigenstate that is largely localized in the first Fock state. The results obtained in Sec. III, and also in Ref. [19], fit this pattern. The increase in the magnitude of the matrix elements in  $\hat{H}(n)$  is not as extreme as in  $\hat{H}_{\text{hierarchical}}$ , especially as we go to higher Fock states. However, our numerical simulations show that for  $n \geq 3$  the states at the center of the spectrum follow the general behaviour produced by the simple example of  $\hat{H}_{\text{hierarchical}}$ . This toy model also provides an intuitive explanation for the seemingly paradoxical situation that occurs for  $n > 4$ , where the dynamics is very sensitive to the parity of  $N$ , even though the photon number remains largely confined to small values, no matter how large  $N$  is.

One might wonder what Q and Wigner functions would be obtained in the dynamics with fractional values of  $n$ . In particular, the phase-space functions shown in Ref. [17] had threefold and fourfold symmetries for the cases  $n = 3$  and  $n = 4$ , respectively. These symmetries are a result of the fact that only multiples of  $n$  photons appear in the quantum state. The symmetry in each pattern does not depend on the exact amplitudes of the different quantum states. Since we do not have a simple mapping between the basis states and photon

number states in the case of fractional  $n$ , we cannot construct similar phase-space functions in a straightforward manner.

## V. CONCLUSION

In conclusion, we have generalized calculations of generalized squeezing to include fractional values of the squeezing order  $n$ , which has allowed us to analyze some key features in the spectrum and dynamics associated with generalized squeezing. In particular, using fractional values of  $n$  combined with extrapolation has allowed us to infer results about the computationally challenging cases  $n = 2$  and  $n = 4$ , which are critical points at which qualitative changes in behaviour occur. In addition to its utility as a computational tool to predict the behaviour near such critical points, our approach has also allowed us to deduce intuitive explanations for phenomena related to the continuity of the spectrum and the oscillatory dynamics encountered in the study of generalized squeezing. These results add valuable insight to our understanding of high-order nonlinearity in quantum optics and suggest new methods to study related problems, such as the multi-photon quantum Rabi model.

### Acknowledgments

We would like to thank Mohammad Ayyash and Cid Reyes Bustos for useful discussions. This work was supported by Japan's Ministry of Education, Culture, Sports, Science and Technology (MEXT) Quantum Leap Flagship Program Grant Number JPMXS0120319794.

### Data availability

The datasets generated and/or analysed during the current study are available from the corresponding author on reasonable request.

---

- [1] D. F. Walls and G. J. Milburn, *Quantum Optics* (Springer, Berlin, 1994).
- [2] M. O. Scully and M. S. Zubairy, *Quantum Optics* (Cambridge University Press, 1997).

- [3] P. D. Drummond and M. Hillery, *The Quantum Theory of Nonlinear Optics* (Cambridge University Press, 2014).
- [4] S. Felicetti, D. Z. Rossatto, E. Rico, E. Solano, and P. Forn-Díaz, Two-photon quantum Rabi model with superconducting circuits, *Phys. Rev. A* **97**, 013851 (2018).
- [5] C. W. S. Chang, C. Sabín, P. Forn-Díaz, F. Quijandría, A. M. Vadiraj, I. Nsanzinezza, G. Johansson, and C. M. Wilson, Observation of three-photon spontaneous parametric down-conversion in a superconducting parametric cavity, *Phys. Rev. X* **10**, 011011 (2020).
- [6] A. M. Eriksson, T. Sépulcre, M. Kervinen, T. Hillmann, M. Kudra, S. Dupouy, Y. Lu, M. Khanahmadi, J. Yang, C. Castillo-Moreno, P. Delsing, and S. Gasparinetti, Universal control of a bosonic mode via drive-activated native cubic interactions, *Nature Commun.* **15**, 2512 (2024).
- [7] M. Ayyash, X. Xu, S. Ashhab, and M. Mariantoni, Driven multiphoton qubit-resonator interactions, *Phys. Rev. A* **110**, 053711 (2024).
- [8] O. Băzăvan, S. Saner, D. J. Webb, E. M. Ainley, P. Drmota, D. P. Nadlinger, G. Araneda, D. M. Lucas, C. J. Ballance, and R. Srinivas, Squeezing, trisqueezing, and quadsqueezing in a spin-oscillator system, arXiv:2403.05471.
- [9] S. Saner, O. Băzăvan, D. J. Webb, G. Araneda, D. M. Lucas, C. J. Ballance, and R. Srinivas, Generating arbitrary superpositions of nonclassical quantum harmonic oscillator states, arXiv:2409.03482.
- [10] R. A. Fisher, M. M. Nieto and V. D. Sandberg, Impossibility of naively generalizing squeezed coherent states, *Phys. Rev. D* **29**, 1107 (1984).
- [11] M. Hillery, M. S. Zubairy, and K. Wódkiewicz, Squeezing in higher order nonlinear optical processes, *Phys. Lett. A* **103**, 259 (1984).
- [12] C. K. Hong and L. Mandel, Higher-order squeezing of a quantum field, *Phys. Rev. Lett.* **54**, 323 (1985).
- [13] S. L. Braunstein and R. I. McLachlan, Generalized squeezing, *Phys. Rev. A* **35**, 1659 (1987).
- [14] S. L. Braunstein and C. M. Caves, Phase and homodyne statistics of generalized squeezed states, *Phys. Rev. A* **42**, 4115 (1990).
- [15] M. Hillery, Photon number divergence in the quantum theory of n-photon down conversion, *Phys. Rev. A* **42**, 498 (1990).
- [16] D. Braak, The  $k$ -photon quantum Rabi model, to appear in T. Takagi *et al.* (Eds.),

*Mathematical Foundations for Post-Quantum Cryptography* (Springer, Singapore, 2026); arXiv:2401.02370.

- [17] S. Ashhab and M. Ayyash, Properties and dynamics of generalized squeezed states, *New J. Phys.* **27**, 054104 (2025).
- [18] R. Gordillo and R. Puebla, Comment on “Properties and dynamics of generalized squeezed states”, arXiv:2507.12250.
- [19] S. Ashhab, F. Fischer, D. Lonigro, D. Braak, and D. Burgarth, Finite-dimensional approximations of generalized squeezing, *Phys. Rev. A* **113**, 013703 (2026).
- [20] F. Fischer, D. Burgarth, and D. Lonigro, Self-adjoint realizations of higher-order squeezing operators, arXiv:2508.09044.
- [21] S. Ashhab and M. Ayyash, Reply to Comment on “Properties and dynamics of generalized squeezed states”, arXiv:2601.07227.
- [22] N. Laskin, Fractional Quantum Mechanics, *Phys. Rev. E* **62**, 3135 (2000).
- [23] R. Herrmann, *Fractional Calculus: An Introduction for Physicists* (World Scientific, Singapore, 2011).
- [24] N. Goldenfeld, *Lectures On Phase Transitions And The Renormalization Group* (Taylor & Francis, Boca Raton, 1992).